The Journal of Experimental Biology 200, 713–721 (1997)
Printed in Great Britain © The Company of Biologists Limited 1997
JEB0592

HOW DOES THE CONTRACTILE VACUOLE OF *PARAMECIUM MULTIMICRONUCLEATUM* EXPEL FLUID? MODELLING THE EXPULSION MECHANISM

YUTAKA NAITOH*, TAKASHI TOMINAGA, MASAKI ISHIDA, AGNES K. FOK, MARILYNN S. AIHARA AND RICHARD D. ALLEN

Pacific Biomedical Research Center and Department of Microbiology, Snyder Hall 306, University of Hawaii at Manoa, 2538 The Mall, Honolulu, HI 96822, USA

Accepted 21 November 1996

Summary

To examine the forces needed for discharge of the fluid contents from the contractile vacuole of *Paramecium multimicronucleatum*, the time course of the decrease in vacuole diameter during systole (the fluid-discharging period) was compared with that of various vacuole discharge models. The observed time course did not fit that predicted by a model in which contraction of an actin–myosin network surrounding the vacuole caused discharge nor that predicted by a model in which the surface tension of the lipid bilayer of the vacuole caused discharge. Rather, it fitted that predicted by a model in which the cell's cytosolic pressure was responsible for discharge. Cytochalasin B, an effective inhibitor of actin polymerization, had no effect on the *in vivo* time course of systole. An injection of a monoclonal antibody raised against the proton pumps of the decorated spongiomes (now known to be the locus of fluid segregation in *P. multimicronucleatum*) disrupted the decorated spongiomes and reduced the rate of fluid segregation, whereas it did not alter the time course of systole. We conclude that in *P. multimicronucleatum* the internal pressure of the contractile vacuole is caused predominantly by the cytosolic pressure and that the fluid-segregation mechanism does not directly affect the fluid-discharge mechanism. Elimination of this cytosolic pressure by rupturing the cell revealed the presence of a novel fluid-discharge mechanism, apparently centered in the vacuole membrane. The involvement of tubulation of the vacuole membrane as the force-generating mechanism for fluid discharge in disrupted cells is discussed.

Key words: *Paramecium multimicronucleatum*, contractile vacuole, fluid discharge rate, fluid discharge models.

Introduction

The contractile vacuole is the organelle responsible for osmoregulation in many protozoa (Kitching, 1956) and freshwater sponges (Jepps, 1947). Kitching (1952, 1956, 1967), in pioneering studies on the physiology of the contractile vacuole, pointed out that a pressure on, or a tension at, the vacuole membrane could produce the pressure required to discharge the fluid contents of the vacuole through the vacuole pore.

On the basis of their analysis of cinematographically recorded pulsating contractile vacuoles in *Amoeba proteus*, Wigg *et al.* (1967) argued that the vacuole fluid is discharged by the pressure produced by the cytosolic gel surrounding the vacuole and not by contraction of the vacuole membrane or its associated cytoskeletal elements. They therefore introduced the term 'water expulsion vesicle' to replace the term 'contractile vacuole'. This work provoked a long-standing debate on whether an active contractile process in the vacuole membrane (or a joint membrane–cytoskeletal system) is involved in the pulsation of the vacuole in amoebae and ciliates or whether other forces cause fluid discharge (Patterson, 1977, 1980).

Recently, Doberstein *et al.* (1993) demonstrated that, when antibodies raised against a synthetic peptide with the sequence of the myosin-IC phosphorylation site were introduced into a living *Acanthamoeba* sp., these antibodies interfered with the activity of its contractile vacuole. They suggested that myosin-IC is involved in generating the force required to empty the vacuole in this cell.

Recent exocytosis studies of smaller vesicles have focused on the very early events of pore formation and on the first escape of the vesicle contents to the cell's exterior. The use of patch-clamp techniques demonstrated a 'flickering' type of exocytotic discharge of neurotransmitter substances through a forming pore even before stable membrane fusion has occurred (Alvarez de Toledo *et al.* 1993; Fernández *et al.* 1984; Neher, 1993). It has usually been assumed, for small vesicles, that the

*e-mail: naitoh@pbrc.hawaii.edu.

vesicular contents are expelled by diffusion. These assumptions have now been questioned by Khanin *et al.* (1994) and Parnas and Parnas (1994), who have reported that even for small vesicles in fast synapses the discharge is too rapid to be due solely to diffusion.

In the light of such reports, it seems expedient to re-examine the forces required to expel the exocytotic contents from vesicles of a wide range of diameters. For this study, we chose the contractile vacuole of *P. multimicronucleatum*, which is large enough to allow accurate determination of the time course of the change in vesicle diameter during systole, a variable essential for examining the putative forces that could lead to discharge of the fluid contents. We propose several plausible models by which this pressure may be generated and test how well each model corresponds to the actual observed rate of fluid discharge.

Materials and methods

Cells of *Paramecium multimicronucleatum* (syngen 2) (Allen *et al.* 1988) were grown in an axenic culture medium (Fok and Allen, 1979) and were harvested at the mid-logarithmic phase of growth. These cells were washed with a standard saline solution containing (final concentration in mmol l^{-1}): 0.5 NaCl, 2.0 $CaCl_2$, 1.0 $MgCl_2$, 1.0 KCl and 1.0 Tris–HCl buffer (pH 7.4). Cells were then transferred into each experimental solution and equilibrated in the solution for more than 30 min prior to experimentation. The experimental solutions were prepared by adding the chemicals to be tested (80 mmol l^{-1} sorbitol, 33 μg ml^{-1} cationized ferritin and 0.29 mmol l^{-1} cytochalasin B) to the standard saline solution.

Equilibrated cells were slightly compressed in a thin (20 μm) space between a glass slide and a coverslip. Profile views of the contractile vacuole were video-recorded (Panasonic AG-6300) at 30 frames s^{-1} using a phase-contrast objective (Olympus 40×). The time course of the change in vacuole diameter during systole was measured directly from recorded images of the vacuole displayed frame by frame on a monitor screen. The contractile vacuole is almost spherical in the early and middle phases of systole. In the late phase of systole, it takes on a shape more like an 'Erlenmeyer flask' owing to the presence of microtubules that extend from the pore region and pass over the part of the vacuole next to the pore (Hausmann and Allen, 1977). Therefore, we omitted measurements of the diameter of the vacuole in very late systole.

For fluorescence microscopical examination of the contractile vacuole complex of *P. multimicronucleatum*, formaldehyde-fixed (3 % in 50 mmol l^{-1} phosphate buffer; pH 7.4) and cold (–20 °C)-acetone-permeabilized cells were treated using two monoclonal antibodies, one raised against the decorated spongiome (DS-1) and the other raised against a pool of membranes including the smooth spongiome and the plasma membrane (SS-1) (Allen *et al.* 1990). This incubation was followed by an incubation in fluorescein-isothiocyanate-(FITC)- and Texas-Red-conjugated rabbit anti-mouse IgG and IgM (Miles Laboratories, Naperville, IL, USA), respectively. Unbound antibodies were washed away using excess buffer solution. The cells were observed using a Zeiss microscope equipped with epifluorescence illumination and filters appropriate for FITC (decorated spongiome) (B-2E, Nikon) and for Texas Red (smooth spongiome) (Texas Red filter, Zeiss). Photographs were obtained using photographic film (Kodak Tri-X film) (Fok *et al.* 1995). Intracellular injection of the antibody, DS-1 or IgG_{2b}, was performed as described previously (Ishida *et al.* 1993).

A cell in a small droplet of standard saline solution was fixed instantaneously by squirting a fixative containing 2 % glutaraldehyde against the cell through a fine pipette placed close to the cell. The precise moment of fixation was monitored using a video camera, and the phase of systole was determined. Conventional techniques were employed for obtaining the subsequent electron micrographs (Allen and Fok, 1988). All experiments were performed at a room temperature ranging from 24 to 26 °C.

Results and discussion

The change in the diameter of the contractile vacuole during systole in normal cells

Fig. 1 shows three representative plots of the change in diameter (*D*) during systole (filled circles) of contractile vacuoles with three different initial diameters (the diameter immediately before the start of systole). These contractile vacuoles were from three different cells equilibrated in three different solutions. The initial diameter was largest in the cell equilibrated in saline solution containing 33 μg ml^{-1} cationized ferritin (A; 24.0 μm) and smallest in saline solution containing 80 mmol l^{-1} sorbitol (C; 8.0 μm). In standard saline solution (B), the initial diameter of the contractile vacuole was 14.6 μm. Consecutive video images of the contractile vacuole in the ferritin-exposed cell are shown in the upper portion of Fig. 1.

Modeling the forces that lead to fluid discharge from the vacuole

If the pressure needed for discharge of the contractile vacuole is caused by a tension at the vacuole membrane generated by activation of a myosin–actin-type of contractile network surrounding the vacuole, the contractility of the network would need to be isotropic to keep the vacuole spherical during discharge of its fluid contents. The force along a given great circle on such a spherical vacuole generated by activation of myosin–actin cross-bridges is assumed to be proportional to the number of activated bridges along the circle (Gordon *et al.* 1966). This number is proportional to the product of the density of the cross-bridges and the circumference of the circle. The tension *T* in the network generated by contraction can, therefore, be written as:

$$T = \kappa \frac{n}{S} \pi D , \qquad (1)$$

where *D* is the diameter of the vacuole, *n* is the total number of activated myosin–actin cross-bridges in the network (*n* is assumed to be constant if equal numbers of cross-bridges in

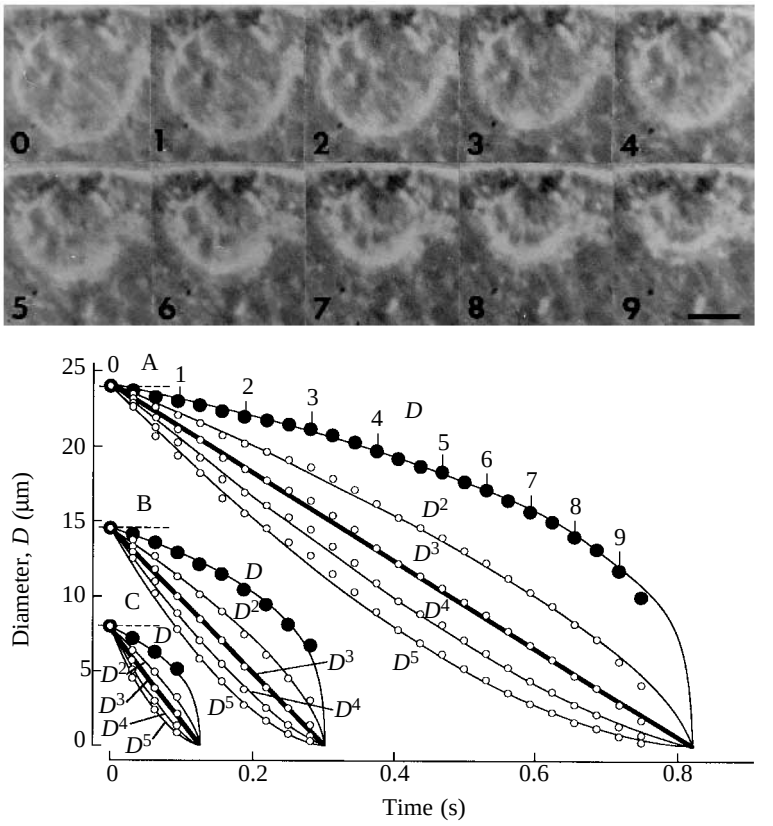

Fig. 1. Change in the contractile vacuole diameter (D, filled circles) in three *Paramecium multimicronucleatum* during systole and for three different external ionic and osmotic conditions (A–C). (A) Standard saline solution containing 33 μg ml^{-1} cationized ferritin, (B) standard saline solution, (C) standard saline solution containing 80 mmol l^{-1} sorbitol. Time t=0 corresponds to the start of systole. Open circles along lines labeled D^2, D^3, D^4 and D^5 are the D values to the second, third, fourth and fifth powers plotted against time, respectively. The straight lines are linear regressions fitted to all points for D^3 (N=25, r^2=0.999 for A; N=10, r^2=0.998 for B; N=4, r^2=0.996 for C). Smooth lines for other plots are drawn according to the values derived from the corresponding straight lines for D^3 *versus* t plots. The horizontal broken line in A corresponds to 24 μm, (24 μm)^2, (24 μm)^3, (24 μm)^4 and (24 μm)^5 for the D, D^2, D^3, D^4 and D^5 plots, respectively, at time 0. Similarly, the broken line in B corresponds to 14.6 μm, (14.6 μm)^2, (14.6 μm)^3, (14.6 μm)^4 and (14.6 μm)^5 for the D, D^2, D^3, D^4 and D^5 plots, respectively, at time 0. The broken line in C corresponds to 8 μm, (8 μm)^2, (8 μm)^3, (8 μm)^4 and (8 μm)^5 for the D, D^2, D^3, D^4 and D^5 plots, respectively, at time 0. The photographs in the upper portion of the figure are consecutive video images of a contractile vacuole corresponding to the D *versus* t plot in A. Each photograph was taken at the time corresponding to the number indicated on the plot. Scale bar, 10 μm.

the network are activated at any one time), S is the surface area of the vacuole membrane and κ is a constant that relates to the force generated by a single cross-bridge.

According to the law of Hagen and Poiseuille, the rate of fluid discharge from the vacuole can be formulated as:

$$-\frac{dV}{dt} = \gamma P, \tag{2}$$

where V is the volume of the vacuole, t is time and P is the internal pressure of a vacuole with reference to the external pressure. If we assume that the pore size does not change during systole, γ can be written as:

$$\gamma = \frac{\pi R^4}{8\eta L}, \tag{3}$$

where R is the radius of the cross section of the pore, L is the length of the pore and η is the viscosity of the fluid. According to McKanna (1973), the pore is almost cylindrical, and R and L are approximately 0.5 μm and 1.2 μm, respectively. η is assumed to be equal to the value for water (1×10^{-3} N m^{-2} s). The value for γ therefore approximates 2.1×10^{-17} N^{-1} m^5 s^{-1}.

The relationship between P and T in a membrane-bound spherical vacuole is given by the Laplace formula as:

$$P = \frac{4T}{D}. \tag{4}$$

The internal pressure generated by the tension can, therefore, be written as:

$$P = \frac{4\kappa n}{D^2}. \tag{5}$$

The rate of the contraction-mediated discharge of the vacuole contents can be formulated as:

$$-\frac{dV}{dt} = \frac{4\gamma\kappa n}{D^2}. \tag{6}$$

A solution of equation 6 (see Appendix) is:

$$D_0^5 - D^5 = \frac{40\gamma\kappa n}{\pi} t, \tag{7}$$

where D_0 is the initial diameter (the diameter at time 0) and D is the diameter at time t. Equation 7 implies that D^5 is proportional to t. This model will be termed the 'contraction model'.

If we assume that the tension at the vacuole surface (T) is due only to the interfacial tension (the surface tension, T_m) of a phospholipid bilayer, a major component of the vacuole membrane, T will be constant (T=T_m) (Harvey, 1954). The rate of discharge, in this case, can be written as:

$$-\frac{dV}{dt} = \gamma \frac{4T_m}{D}. \tag{8}$$

A solution of equation 8 (see Appendix) is:

$$D_0^4 - D^4 = \frac{32\gamma T_m}{\pi} t . \quad (9)$$

Equation 9 implies that D^4 is proportional to t. This model will be termed the 'surface tension model'.

Another plausible source of the internal pressure is cytosolic pressure or turgor. If the cytosolic pressure (P_c) is the sole source, the internal pressure P is assumed to be constant ($P=P_c$) under a given external osmotic condition. The rate of discharge is, therefore, written as:

$$-\frac{dV}{dt} = \gamma P_c . \quad (10)$$

A solution of equation 10 (see Appendix) is:

$$D_0^3 - D^3 = \frac{6\gamma P_c}{\pi} t , \quad (11)$$

which implies that D^3 is proportional to t. This model will be termed the 'cytosolic pressure model'.

Comparison of the time course of change in the vacuole diameter in normal cells with that predicted by each model

To examine which of the three proposed models fits the *in vivo* decrease in vacuole diameter best, values for D^3, D^4 and D^5 were plotted against time (Fig. 1). It is clear that the D^3 *versus* t plot was linear (Fig. 1, thick lines) for all initial vacuole diameters. This implies that the cytosolic pressure model most accurately describes the contractile vacuole *in vivo*, i.e. the fluid contents of the contractile vacuole of *P. multimicronucleatum* are expelled by the cytosolic pressure.

The values for the rate of discharge determined from the slopes of D^3 *versus* t in Fig. 1 were $8.9\times10^3\,\mu m^3\,s^{-1}$ for A, $5.4\times10^3\,\mu m^3\,s^{-1}$ for B and $2.0\times10^3\,\mu m^3\,s^{-1}$ for C. The rate was higher for larger vacuoles, which implies that the effective diameter of the contractile vacuole pore is larger in larger vacuoles. We found that the rate of discharge was proportional to D_0^2 (data not shown). The values for the rate of discharge after equilibration in four different external solutions (standard saline solution, saline containing 80 mmol l^{-1} sorbitol or 33 μg ml^{-1} cationized ferritin and axenic culture medium) are shown in Table 1. The normalized value for the rate of discharge was only significantly affected by the cationized-ferritin-containing saline solution (see below), implying that the cytosolic pressure remains approximately constant in the different external solutions used. The internal pressure of the vacuole was calculated from the rate of discharge in standard saline solution, according to the Law of Hagen and Poiseuille, to be approximately 2.0×10^2 N m^{-2} from control values for the 80 mmol l^{-1} sorbitol and ferritin experiments shown in Table 1.

Table 1. *Contractile vacuole activities in* Paramecium multimicronucleatum *under different conditions*

Condition		Initial diameter, D_0 (μm)	$10^3\times$ Rate of discharge ($\mu m^3\,s^{-1}$)	Pulsation frequency (min^{-1})	Rate of fluid segregation ($\mu m^3\,s^{-1}$)
Injection of monoclonal	E	10.3±0.7 (16)	4.7±0.2 (6)	3.7±0.6 (16)*	27.3±3.9 (16)*
antibody, DS-1	C	10.8±0.3 (16)	4.2±0.4 (7)	5.6±0.5 (16)	60.1±6.2 (16)
Equilibration in 80 mmol l^{-1}	E	7.7±0.9 (28)*	4.6±0.2 (8)	1.2±0.2 (28)*	9.9±2.3 (28)*
sorbitol solution	C	13.3±0.5 (32)	4.2±0.3 (7)	3.6±0.3 (32)	71.8±5.1 (32)
Equilibration in 33 μg ml^{-1}	E	24.4±2.1 (34)*	3.0±0.6 (7)*	1.6±0.3 (34)*	78.0±8.3 (20)
cationized ferritin solution	C	12.5±0.3 (28)	4.3±0.3 (8)	4.9±0.3 (28)	79.9±6.4 (28)

Values are means ± S.D.

E, experimental data obtained from cells treated as indicated; C, control data. Data in each E/C pair for each condition were obtained from cells from the same culture.

Asterisks indicate a significant difference between values in an E/C pair ($P<0.05$).

The monoclonal antibody injection experiments were performed in axenic culture medium (Fok and Allen, 1979). Control values for these experiments were obtained using cells injected with IgG_{2b} instead of DS-1. Control values for the experiments using 80 mmol l^{-1} sorbitol or 33 μg ml^{-1} of cationized ferritin solution were obtained from cells equilibrated in standard saline solution.

The rates of discharge data were normalized to a vacuole diameter of 12 μm.

The rate of fluid segregation was obtained by dividing the volume of the contractile vacuole immediately before the start of systole by the time from the end of the previous systole.

In the experiments using 80 mmol l^{-1} sorbitol solution, if the contractile vacuole did not appear for more than 3 min, D_0, the pulsation frequency and the rate of segregation were regarded as 0.

In the experiments using 33 μg ml^{-1} cationized ferritin solution, when the contractile vacuole did not show a systole for more than 3 min, the diameter at the end of the observation was regarded as D_0 and the pulsation frequency was regarded as 0.

For some large contractile vacuoles, the rate of fluid segregation could be calculated from the change in volume during this 3 min period.

For the rate of discharge data, E and C values may result from cells at different stages of volume regulation (Patterson, 1980), especially in the case of the sorbitol solution. Multiple causes for changes in the rate of discharge would be expected, although we cannot define these clearly at present.

Effect of external application of cytochalasin B on the rate of discharge

In order to examine further the possibility of involvement of an actin-mediated contractile process in the discharge of vacuole fluid, we determined the effects of external application of 0.29 mmol l^{-1} cytochalasin B (a potent inhibitor of actin polymerization) on the rate of fluid discharge from the vacuole. This drug did not alter the rate of discharge ($4.6\times10^3\pm0.8\times10^3$ $\mu m^3 s^{-1}$, N=10, compared with the control rate of $4.6\times10^3\pm0.8\times10^3$ $\mu m^3 s^{-1}$, N=7) or the linear D^3 *versus* t relationship, although it inhibited actin-mediated food vacuole formation in the cells examined (Allen *et al.* 1995; Allen and Fok, 1983). This result indicates that an actin-mediated contractile process involving a membrane-associated cytoskeleton is not involved in the generation of the internal pressure required to expel vacuole fluid in *P. multimicronucleatum*. The lack of any ultrastructural or immunological evidence for the presence of a fibrous network system around the contractile vacuole of *Paramecium* (Allen and Fok, 1988, for *P. multimicronucleatum*; Cohen *et al.* 1984, for *P. caudatum*) that could account for contraction of the vacuole is also consistent with this finding.

The relationship between the fluid-discharge mechanism and the fluid-segregation mechanism in the contractile vacuole complex

The fluid-segregation mechanism of the contractile vacuole complex in *P. multimicronucleatum* is situated in the decorated spongiomes (Allen *et al.* 1990). To determine whether this mechanism affects the mechanism used to generate the fluid-expulsion force, fluid discharge was examined in cells in which fluid segregation had been partially blocked by injection of a monoclonal antibody (DS-1) raised against the decorated spongiomes in *P. multimicronucleatum* (Ishida *et al.* 1993). As shown in Table 1, injection of this antibody reduced the rate of fluid segregation by approximately 55 % and the pulsation frequency by approximately 34 %, which resulted in a sharp reduction in the total fluid output from these cells. In spite of this functional retardation of fluid segregation, the linear D^3 *versus* t relationship and the rate of fluid expulsion during systole were not affected (Table 1).

Morphological changes correlated with functional retardation of the fluid-segregation mechanism in response to injection of DS-1 were sought using fluorescence microscopy. Fig. 2B shows representative micrographs of a cell injected with DS-1 and Fig. 2A shows a control cell injected with nonspecific IgG_{2b}, an immunoglobulin of the same serotype as monoclonal antibody DS-1. The micrographs clearly demonstrate that the decorated spongiomes were markedly disrupted by DS-1. This result is consistent with our previous observations (Ishida *et al.* 1993).

Increased external osmolarity caused by the addition of 80 mmol l^{-1} sorbitol to the standard saline solution resulted in decreases in D_0, pulsation frequency and rate of fluid segregation (Table 1), which together resulted in a pronounced

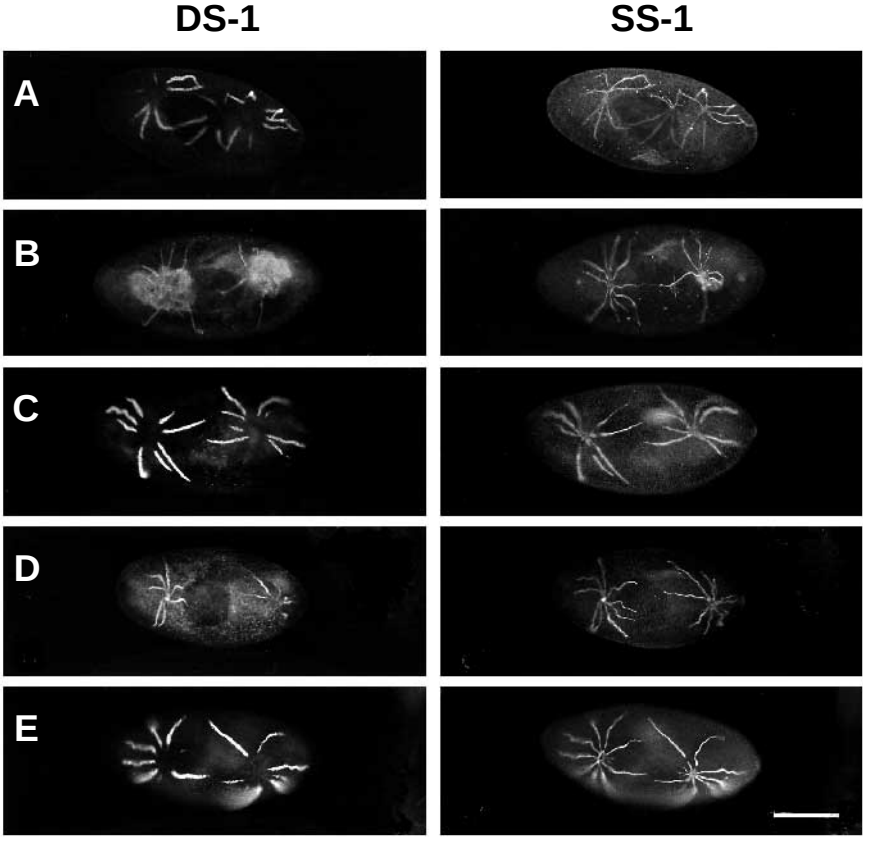

Fig. 2. Fluorescence microscope images of cells of *Paramecium multimicronucleatum* double-exposed to two monoclonal antibodies. The decorated spongiome is revealed by reaction with monoclonal antibody DS-1 (an IgG) (first column); the smooth spongiome is revealed by reaction with monoclonal antibody SS-1 (an IgM) (second column). (A) IgG_{2b}-injected cell. (B) DS-1 injected cell. (C) Standard saline solution. (D) Standard saline containing 80 mmol l^{-1} sorbitol. (E) Standard saline containing 33 $\mu g\,\mu l^{-1}$ cationized ferritin. Scale bar, 50 μm.

decrease in the total fluid output by the cell. However, the linearity of the D^3 *versus t* relationship (Fig. 1) and the rate of fluid discharge during systole (Table 1) were not affected. Using fluorescence microscopy, the label for the decorated spongiomes, but not the smooth spongiomes, was markedly reduced in cells placed in the sorbitol-containing saline (compare Fig. 2D with Fig. 2C) (Ishida *et al.* 1996).

Cationized ferritin ($33\,\mu g\,ml^{-1}$) added to standard saline solution caused a significant increase in D_0 and decrease in the pulsation frequency. However, the rate of fluid segregation over the relatively short duration of the experiments was unaffected by the presence of cationized ferritin (Table 1). This is consistent with the observation that the decorated spongiome was little affected by the presence of cationized ferritin (compare Fig. 2E with Fig. 2C). It should be noted, however, that the normalized rate of fluid discharge during systole was significantly reduced by cationized ferritin even though the linearity of the D^3 *versus t* relationship remained unchanged (Fig. 1). The lower rate of discharge could correspond to a decrease in the functional diameter of the pore. We assume that cationized ferritin somehow inhibits the mechanism of pore opening, in which fusion of the vacuole membrane with the pore membrane is critical.

It should be noted that morphological and physiological disruption of the fluid-segregation mechanism has little effect on the linearity of the D^3 *versus t* relationship. This observation strongly supports the hypothesis that the fluid-segregation mechanism *per se* is not intimately tied to the mechanism for generating the internal pressure of the contractile vacuole used to expel the fluid.

Change in vacuole diameter during systole in mechanically ruptured cells and comparison with the predictions of the models

It is assumed that the cell's cytosolic pressure is greatly reduced or effectively eliminated by rupturing the cell. We therefore examined the effects of cell rupture on the time course of the change in vacuole diameter during systole. Cells equilibrated in standard saline solution and placed in a thin space formed between a glass slide and a coverslip were gradually squeezed by pushing the coverslip against the glass slide using a micromanipulator, until the cells were flattened and eventually ruptured. In some cases, the contractile vacuole of the disrupted cell underwent systole after cell rupture.

Fig. 3 gives two representative graphs showing the change in diameter during systole of two contractile vacuoles with different initial diameters (22.9 μm in A and 14.3 μm in B) derived from two different ruptured cells. Values calculated for D^2, D^3, D^4 and D^5 are also shown. Consecutive video images of the larger vacuole are shown in the upper portion of the figure.

The period of systole in contractile vacuoles from ruptured cells was markedly prolonged. The plot of D^2 *versus t* was always linear irrespective of the initial diameter of the vacuole (thick lines in Fig. 3), whereas the D^2 *versus t* plots for contractile vacuoles in unruptured cells were distinctly curved (Fig. 1). These results suggest that the cytosolic pressure model is no longer applicable to contractile vacuoles after cell rupture. Electron micrographs of cells fixed immediately after disruption demonstrate a clear rupture of the surface membrane and outflow of a considerable amount of cytosol through the rupture (data not shown). Disruption undoubtedly brings about a sudden reduction in cytosolic pressure.

A novel mechanism for fluid discharge in ruptured cells

As described above, contractile vacuoles from ruptured cells showed systole with a time course that differed from that predicted by any of the models presented in equations 7, 9 and 11. This suggests the presence of a novel mechanism for fluid discharge in ruptured cells.

The D^2 *versus t* line can be formulated as:

$$D_0^2 - D^2 = \alpha t\,, \tag{12}$$

where α is the slope of the line. Equation 12 implies that the rate of decrease in the vacuole's membrane area ($\pi\alpha/4$) is constant during vacuole discharge. There is strong morphological evidence, at least in ciliates, to show that the membrane of the contractile vacuole *in vivo* is transformed during systole into tubules that do not separate from the vacuole membrane (Allen and Fok, 1988). An electron micrograph showing this kind of membrane tubulation in a ruptured cell is presented in Fig. 4. Although the mechanism for transformation of an approximately planar membrane into tubules is not completely understood, the rate of this physical event is assumed to be constant under a given physical condition. Such tubulation would presumably lead to a constant reduction in the vacuole membrane area surrounding the undischarged fluid.

If we assume a model in which the vacuole membrane tension is proportional to the vacuole membrane area, the tension can be written as:

$$T = \beta\pi D^2\,, \tag{13}$$

where β is a constant which represents the tension per unit membrane area. The internal pressure P can then be formulated as:

$$P = 4\beta\pi D\,. \tag{14}$$

The rate of discharge of the vacuole contents will be:

$$-\frac{\mathrm{d}V}{\mathrm{d}t} = 4\beta\gamma\pi D\,. \tag{15}$$

A solution of equation 15 (see Appendix) is:

$$D_0^2 - D^2 = 16\beta\gamma t\,. \tag{16}$$

Equation 16 implies that D^2 is proportional to t. This model will be termed the 'membrane area-proportional tension model'. This model fits the observed change in contractile vacuole diameter in ruptured cells and suggests that there is a causal relationship between membrane tubulation and the membrane area-proportional tension.

The bending energy stored in the vacuole membrane and the work done by the vacuole to discharge the fluid

It is conceivable that some of the energy used to move fluid

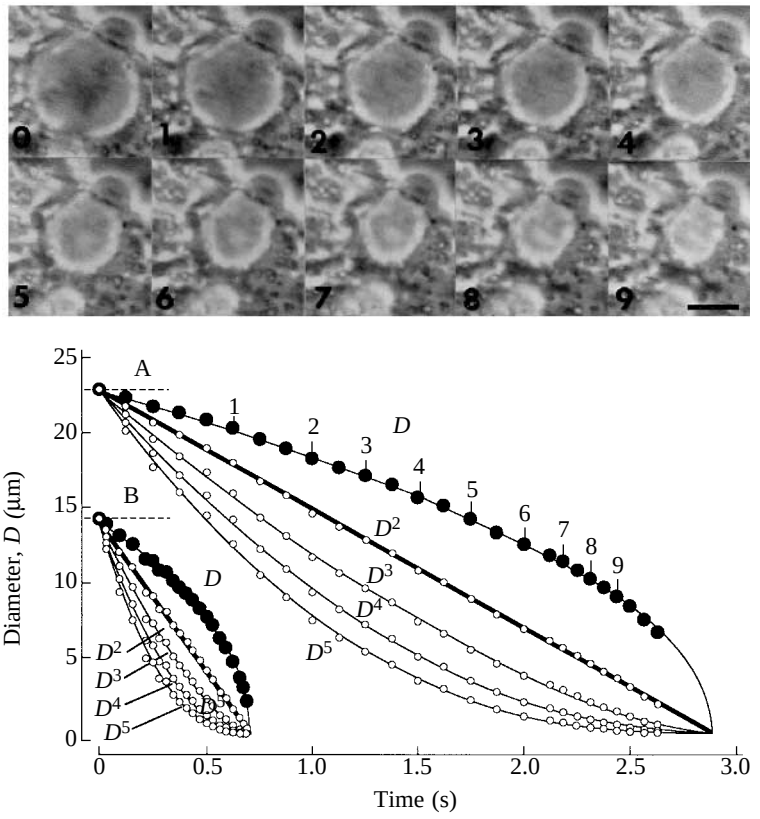

Fig. 3. Change in the diameter (D) of contractile vacuoles from mechanically ruptured cells of *Paramecium multimicronucleatum* during systole in standard saline solution (filled circles). (A) A large vesicle (diameter 22.9 μm at time t=0). (B) A smaller vesicle (diameter 14.3 μm at time t=0). Open circles along lines labeled D^2, D^3, D^4 and D^5 are the D values to the second, third, fourth and fifth powers plotted against time, respectively. The thick straight lines are linear regressions fitted to all points for D^2 (N=26, r^2=1.000 for A; N=21, r^2=0.999 for B). Smooth lines for other plots are drawn according to the values derived from the straight line for the D^2 *versus* t plots. The horizontal broken line in A corresponds to 22.9 μm, $(22.9\,\mu m)^2$, $(22.9\,\mu m)^3$, $(22.9\,\mu m)^4$ and $(22.9\,\mu m)^5$ for D, D^2, D^3, D^4 and for D^5 plots at t=0, respectively. The horizontal broken line in B corresponds to 14.3 μm, $(14.3\,\mu m)^2$, $(14.3\,\mu m)^3$, $(14.3\,\mu m)^4$ and $(14.3\,\mu m)^5$ for D, D^2, D^3, D^4 and for D^5 plots, respectively. The photographs in the upper portion of the figure are consecutive video images of a contractile vacuole corresponding to the D *versus* t plots in A. Each photograph was taken at the time corresponding to the number indicated on the plot. Scale bar, 10 μm.

into the decorated spongiomes and to expand the tubular system into a vacuole would be stored in the approximately planar vacuole membrane as bending (elastic) energy. When the pore opens, this energy would be released to aid in expelling the vacuole contents. We therefore estimated the work done by the two vacuoles shown in Fig. 3 to discharge

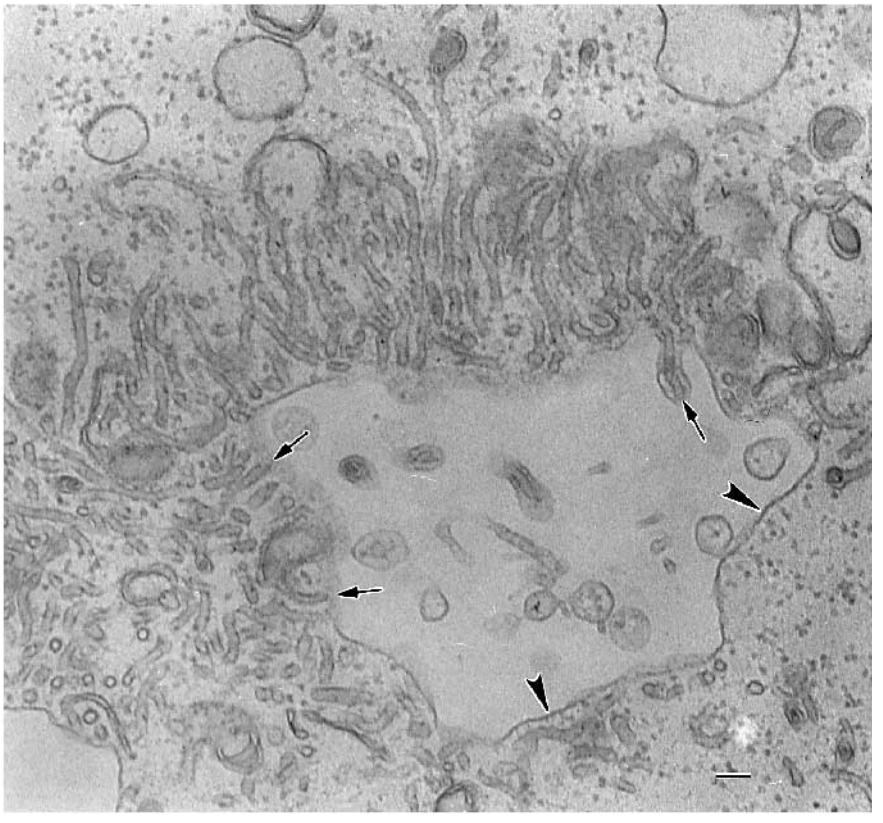

Fig. 4. Electron micrograph of the contractile vacuole membrane in a ruptured cell of *Paramecium multimicronucleatum* during late systole. The usually approximately planar vacuole membrane (arrowheads) is transformed into a network of 40 nm tubules (arrows). Scale bar, 100 nm.

the fluid. The law of Hagen and Poiseuille and equation 12 together give:

$$P = \frac{\alpha\pi}{4\gamma} D \,. \qquad (17)$$

The work done can be written as:

$$-\int_{V_0}^{0} P\mathrm{d}V = \frac{\alpha\pi^2}{32\gamma} {D_0}^4 \,, \qquad (18)$$

where V_0 is the vacuole volume immediately before the start of discharge. The work done by the vacuoles shown in Fig. 3A,B is therefore 7.4×10^{-13} N m and 1.8×10^{-13} N m, respectively.

These values were compared with values estimated for the bending energy stored in the vacuole membrane. According to Hui and Sen (1989), the bending energy stored in a curved bilayer membrane when it is flattened can be expressed as:

$$\Delta E = 2\delta {S_o}^2 \,, \qquad (19)$$

where ΔE is the energy stored per unit area, δ is the bending modulus of the membrane and S_o is the curvature of the membrane. Although this formula is intended for isotropic curvature, we applied it, taking a value of $0.05\ \mathrm{nm}^{-1}$ for the curvature of the membrane obtained from the reciprocal of the radius of a cross section of the tubule (approximately 20 nm; see Fig. 4). The calculated energy storage values were 7.6×10^{-13} N m for the vacuole shown in Fig. 3A and 3.0×10^{-13} N m for that in Fig. 3B. These values correspond extremely well with the work done by each vacuole determined from the rate of decrease in the volume of the vacuole. This coincidence suggests that the bending energy stored in the flattened vacuole membrane is sufficient to discharge the vacuole contents in ruptured cells as the membrane transforms into tubules.

Does the membrane area-proportional tension facilitate fluid discharge by cytosolic pressure in normal cells?

We clearly demonstrated above that the fluid contents of the *in vivo* contractile vacuole of *P. multimicronucleatum* were discharged by cytosolic pressure and that tension of the vacuole membrane generated in association with membrane tubulation may be responsible for fluid discharge when the cytosolic pressure is eliminated. The rates of discharge calculated from the slope α of the D^2 *versus* t plots shown in Fig. 3 are much lower than those found prior to rupturing the cell and calculated from the slope of the corresponding D^3 *versus* t plots ($4.7\times10^2\ \mu\mathrm{m}^3\,\mathrm{s}^{-1}$ *versus* $4.1\times10^3\ \mu\mathrm{m}^3\,\mathrm{s}^{-1}$ in A and $1.9\times10^3\ \mu\mathrm{m}^3\,\mathrm{s}^{-1}$ *versus* $6.1\times10^3\ \mu\mathrm{m}^3\,\mathrm{s}^{-1}$ in B; D_0 is normalized to 12.0 μm). The times required for complete discharge were calculated from each value for the rate of discharge and found to be 2.9 s *versus* 0.22 s in A and 0.70 s *versus* 0.15 s in B. This indicates that, in a normal (unruptured) cell, tubulation of the vacuole membrane is always preceded by fluid discharge due to cytosolic pressure. Therefore, membrane tubulation is not likely to facilitate fluid discharge *in vivo* where fluid discharge is dependent solely on the cytosolic pressure.

Exocytosis in general

We have described a novel mechanism that may facilitate some types of exocytic discharge. As exocytic vesicles vary in size and content, it is highly probable that some cells and organisms employ mechanisms similar to those described here for the contractile vacuole for discharging their vesicular contents. In addition, forces generated by the bending of the membrane of exocytic vesicles may contribute to the mechanism of exocytosis by causing the membrane to tubulate. These forces should be considered, along with other mechanisms, when the discharge of exocytic contents is under investigation.

Appendix

This section presents the derivation of the equations that appear in the text. Symbols have the same meaning as in the text.

The rate of change of the volume of the contractile vacuole, $\mathrm{d}V/\mathrm{d}t$, can be written as:

$$\frac{\mathrm{d}V}{\mathrm{d}t} = \frac{\mathrm{d}V}{\mathrm{d}D}\frac{\mathrm{d}D}{\mathrm{d}t} = \frac{\pi}{6}\frac{\mathrm{d}D^3}{\mathrm{d}D}\frac{\mathrm{d}D}{\mathrm{d}t} = \frac{\pi}{2} D^2 \frac{\mathrm{d}D}{\mathrm{d}t} \,. \qquad (A1)$$

Equation 6 can, therefore, be written as:

$$-\frac{\pi}{2} D^2 \frac{\mathrm{d}D}{\mathrm{d}t} = \frac{4\gamma\kappa n}{D^2} \,. \qquad (A2)$$

This equation can be solved as follows:

$$-\int D^4 \mathrm{d}D = \frac{8\gamma\kappa n}{\pi} \int \mathrm{d}t + C \,, \qquad (A3)$$

$$-D^5 = \frac{40\,\gamma\kappa n}{} t + C' \,, \qquad (A4)$$

$$D_0{}^5 - D^5 = \frac{40\,\gamma\kappa n}{\pi} t \,. \qquad (A5)$$

Similarly, equation 8 can be solved as follows:

$$-\frac{\pi}{2} D^2 \frac{\mathrm{d}D}{\mathrm{d}t} = \gamma \frac{4T_\mathrm{m}}{D} \,, \qquad (A6)$$

$$-\int D^3 \mathrm{d}D = \frac{8}{\pi}\gamma T_\mathrm{m} \int \mathrm{d}t + C \,, \qquad (A7)$$

$$-D^4 = \frac{32\gamma T_\mathrm{m}}{\pi} t + C' \,, \qquad (A8)$$

$$D_0{}^4 - D^4 = \frac{32\gamma T_\mathrm{m}}{\pi} t \,. \qquad (A9)$$

Similarly, equation 10 can be solved as follows:

$$-\frac{\pi}{2}D^2\frac{\mathrm{d}D}{\mathrm{d}t}=\gamma P_\mathrm{c}\ , \tag{A10}$$

$$-\int D^2\mathrm{d}D=\frac{2\gamma P_\mathrm{c}}{\pi}\int \mathrm{d}t+C\,, \tag{A11}$$

$$-D^3=\frac{6\gamma P_\mathrm{c}}{\pi}t+C'\,, \tag{A12}$$

$$D_0{}^3-D^3=\frac{6\gamma P_\mathrm{c}}{\pi}t\,. \tag{A13}$$

Similarly, equation 15 can be solved as follows:

$$-\frac{\pi}{2}D^2\frac{\mathrm{d}D}{\mathrm{d}t}=4\beta\gamma\pi D\,, \tag{A14}$$

$$-\int D\mathrm{d}D=8\,\beta\gamma\int \mathrm{d}t+C\,, \tag{A15}$$

$$-D^2=16\beta\gamma t+C'\,, \tag{A16}$$

$$D_0{}^2-D^2=16\beta\gamma t\,. \tag{A17}$$

C and C' in the above equations are integration constants for each calculation.

This work was supported by NSF Grant MCB 95 05910. We thank Dr Y. Hiramoto and Dr M. Yoneda for their valuable comments on the modeling and Dr H. Seki and Dr H. Yamagishi for help with the equipment.

References

ALLEN, R. D., BALA, N. P., ALI, R. F., NISHIDA, D. M., AIHARA, M. S., ISHIDA, M. AND FOK, A. K. (1995). Rapid bulk replacement of acceptor membrane by donor membrane during phagosome to phagoacidosome transformation in *Paramecium*. *J. Cell Sci.* **108**, 1263–1274.

ALLEN, R. D. AND FOK, A. K. (1983). Nonlysosomal vesicles (acidosomes) are involved in phagosome acidification in *Paramecium*. *J. Cell Biol.* **97**, 566–570.

ALLEN, R. D. AND FOK, A. K. (1988). Membrane dynamics of the contractile vacuole complex of *Paramecium*. *J. Protozool.* **35**, 63–71.

ALLEN, R. D., UENO, M. S. AND FOK, A. K. (1988). A survey of lectin binding in *Paramecium*. *J. Protozool.* **35**, 400–407.

ALLEN, R. D., UENO, M. S., POLLARD, L. W. AND FOK, A. K. (1990). Monoclonal antibody study of the decorated spongiome of contractile vacuole complexes of *Paramecium*. *J. Cell Sci.* **96**, 469–475.

ALVAREZ DE TOLEDO, G., FERNÁNDEZ-CHACÓN, R. AND FERNÁNDEZ, J. M. (1993). Release of secretory products during transient vesicle fusion. *Nature* **363**, 554–558.

COHEN, J., GARREAU DE LOUBRESSE, N. AND BEISSON, J. (1984). Actin microfilaments in *Paramecium*: localization and role in intracellular movements. *Cell Motil.* **4**, 443–468.

DOBERSTEIN, S. K., BAINES, I. C., WIEGAND, G., KORN, E. D. AND POLLARD, T. D. (1993). Inhibition of contractile vacuole function *in vivo* by antibodies against myosin-I. *Nature* **365**, 841–843.

FERNÁNDEZ, J. M., NEHER, E. AND GOMPERTS, B. D. (1984). Capacitance measurements reveal stepwise fusion events in degranulating mast cells. *Nature* **312**, 453–455.

FOK, A. K., AIHARA, M. S., ISHIDA, M., NOLTA, K. V., STECK, T. L. AND ALLEN, R. D. (1995). The pegs on the decorated tubules of the contractile vacuole complex of *Paramecium* are proton pumps. *J. Cell Sci.* **108**, 3163–3170.

FOK, A. K. AND ALLEN, R. D. (1979). Axenic *Paramecium caudatum*. I. Mass culture and structure. *J. Protozool.* **26**, 463–470.

GORDON, A. M., HUXLEY, A. F. AND JULIAN, F. J. (1966). The variation in isometric tension with sarcomere length in vertebrate muscle fibres. *J. Physiol., Lond.* **184**, 170–192.

HARVEY, E. N. (1954). The tension at the cell surface. In *Protoplasmatologia*, vol. II (ed. L. V. Heilbrunn and F. Weber), E5, pp. 1–30. Vienna: Springer Verlag.

HAUSMANN, K. AND ALLEN, R. D. (1977). Membranes and microtubules of the excretory apparatus of *Paramecium caudatum*. *Eur. J. Cell Biol.* **15**, 303–320.

HUI, S.-W. AND SEN, A. (1989). Effects of lipid packing on polymorphic phase behavior and membrane properties. *Proc. natn. Acad. Sci. U.S.A.* **86**, 5825–5829.

ISHIDA, M., AIHARA, M. S., ALLEN, R. D. AND FOK, A. K. (1993). Osmoregulation in *Paramecium*: the locus of fluid segregation in contractile vacuole complex. *J. Cell Sci.* **106**, 693–702.

ISHIDA, M., FOK, A. K., AIHARA, M. S. AND ALLEN, R. D. (1996). Hyperosmotic stress leads to reversible dissociation of the proton pump-bearing tubules from the contractile vacuole complex in *Paramecium*. *J. Cell Sci.* **109**, 229–237.

JEPPS, M. W. (1947). Contribution to the study of the sponges. *Proc. R. Soc. Lond. B* **134**, 408–417.

KHANIN, R., PARNAS, H. AND SEGEL, L. (1994). Diffusion cannot govern the discharge of neurotransmitter in fast synapses. *Biophys. J.* **67**, 966–972.

KITCHING, J. A. (1952). Contractile vacuoles. *Symp. Soc. exp. Biol.* **6**, 145–165.

KITCHING, J. A. (1956). Contractile vacuoles of protozoa. In *Protoplasmatologia*, vol. III (ed. L. V. Heilbrunn and F. Weber), D3a, pp. 1–45. Vienna: Springer-Verlag.

KITCHING, J. A. (1967). Contractile vacuoles, ionic regulation and excretion. In *Research in Protozoology*, vol. 1 (ed. T.-T. Chen), pp. 307–336. London: Pergamon Press.

MCKANNA, J. A. (1973). Fine structure of the contractile vacuole pore in *Paramecium*. *J. Protozool.* **20**, 631–638.

NEHER, E. (1993). Secretion without full fusion. *Nature* **363**, 497–498.

PARNAS, H. AND PARNAS, I. (1994). Neurotransmitter release at fast synapses. *J. Membr. Biol.* **142**, 267–279.

PATTERSON, D. J. (1977). On the behaviour of contractile vacuoles and associated structures of *Paramecium caudatum* (Ehrbg). *Protistologica* **13**, 205–212.

PATTERSON, D. J. (1980). Contractile vacuoles and associated structures: their organization and function. *Biol. Rev.* **55**, 1–46.

WIGG, D., BOVEE, E. C. AND JAHN, T. L. (1967). The evacuation mechanism of the water expulsion vesicle (‘contractile vacuole’) of *Amoeba proteus*. *J. Protozool.* **14**, 104–108.